# Complementary Relation between Ion−Counterion and Ion−Solvent Interaction in Lithium Halide−Methanol Solutions

**Tünde Megyes,[†] Tamás Radnai,[†] and Akihiro Wakisaka*[,‡]**

*National Institute of Advanced Industrial Science and Technology (AIST), Onogawa 16-1, Tsukuba, Ibaraki 305-8569, Japan, and Chemical Research Center, Hungarian Academy of Sciences, Budapest, P.O. Box 17, H-1525, Hungary*

*Received: April 22, 2002; In Final Form: June 18, 2002*

Mass spectrometric study on the cluster structure of methanol solutions containing lithium halides (LiX = LiCl, LiBr, and LiI) is reported. Solvated ions: $Li^+(CH_3OH)_n$ and $X^-(CH_3OH)_k$, and salt clusters: $Li^+(Li^+X^-)_s(CH_3OH)_m$ and $X^-(Li^+X^-)_p(CH_3OH)_r$, were observed in the mass spectra. The number of methanol molecules around $Li^+$, especially in $Li^+(Li^+X^-)_s(CH_3OH)_m$ clusters, increased when changing the anions from $Cl^-$ to $I^-$, which suggested that there was a complementary relation between a $Li^+-CH_3OH$ interaction and a $Li^+-X^-$ interaction. In the case of $X^- = I^-$, the $Li^+-CH_3OH$ interaction was enhanced in comparing with the case of $X^- = Cl^-$, because a $Li^+-I^-$ interaction is weaker than a $Li^+-Cl^-$ interaction. This observed complementary relation is a kind of intrinsic property of a liquid phase. Furthermore, mass distribution of the solvated ions and the salt clusters had correlations with physicochemical properties such as solvation energies and molar conductivities.

## Introduction

The structure of solvated ions in solutions has long been an attractive subject for studies by means of spectroscopic and diffraction methods.[1−12] While the methods are very efficient in most cases, the clear separation of the information on the solvated species from the structure of the bulk liquid is sometimes difficult due to the difficulties of experimental data treatment and complexity of the applied models. The models are often derived from dimer or trimer level calculations for isolated ions and are subject to an extended fitting procedure to the experimental data. Accordingly, a new experimental approach may significantly help to overcome the difficulties.

As a new experimental approach to the structures in solution, mass spectrometry of clusters, formed by fragmentation of liquid droplets generated through a bubble-jet method in a vacuum, has been proposed.[13,14] During the fragmentation, the relatively weakly interacting molecules are vaporized and the relatively strongly interacting ones form clusters. It has already been reported that the resulting clusters reflect intermolecular interactions in the liquid droplets, and are related with physicochemical properties in solutions.[15−22] For example, as for non- or weak electrolyte solutions, nonideality of water−methanol and water−acetonitrile mixtures,[15] preferential solvation in aqueous organic solvents,[16−19] and solvation-controlled acid−base molecular self-assembling[20−22] were extensively studied to find out the relation between cluster structures and solution properties.

As a further step, recently, the mass spectrometry for clusters in electrolyte solutions was developed with a combination of an electrospray nozzle interface with a specially designed vacuum system.[23] In our system, the five-stage differentially pumped vacuum system is specially designed to minimize vaporization of solvent molecules from clusters, which distinguishes our method from conventional electrospray ionization mass spectrometers. By applying our technique, we have reported that the difference in molar conductivities of aqueous $HNO_3$ and $H_2SO_4$ can be explained on the basis of the peak intensity ratio of the protonated water clusters to the clusters including nonionized $HNO_3$ or $H_2SO_4$,[24] and that the salt effect on hydrophobic self-aggregation of a nucleoside (cytidine) in water can be demonstrated for NaCl, KCl, and $MgCl_2$ salts.[23] In these experiments, both solvated-ion clusters and ion-pair (or salt) clusters were observed, which made it possible to discuss physicochemical properties of electrolyte solutions at a cluster level.

Here we would like to report study on microscopic structures of lithium halide−methanol solutions through the mass spectrometric analysis of positively and negatively charged clusters. From the observed solvated-ion clusters, salt clusters, and solvated-salt clusters, the complementary relation between ion−counterion and ion−solvent interactions is discussed for a series of LiCl, LiBr, and LiI in methanol. In other words, competition between solvation of ion and ion-pair formation is investigated with varying the counterion. Recently we have reported that the solvation for $Cl^-$ in LiCl−methanol solution was strongly enhanced by the addition of 18-crown-6.[25] Since 18-crown-6 interacted with $Li^+$ predominantly in the solution to reduce $Li^+-Cl^-$ interaction, the enhancement of the solvation for $Cl^-$ by the presence of 18-crown-6 has been reasonably attributed to the decrease of the electrostatic interactions by the counterion $Li^+$. It should be recognized here that the complementary relation among interactions in solutions is one of the general properties of solutions.

In connection with electrospray ion formation mechanism, mass spectrometric analyses of alkali metal halides in methanol or in aqueous methanol have been reported extensively.[26−28] The relative mass abundances of positive and negative ion

* Author to whom correspondence should be addressed. E-mail: akihiro-wakisaka@aist.go.jp.

[†] Chemical Research Center, Hungarian Academy of Sciences.

[‡] National Institute of Advanced Industrial Science and Technology (AIST).

10.1021/jp021028v CCC: $22.00 
Published on Web 08/09/2002

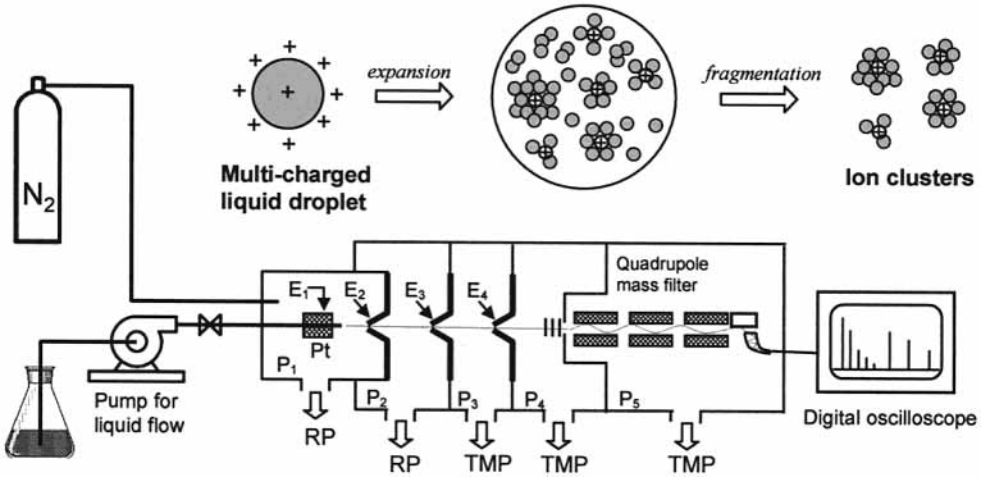


**Figure 1.** A schematic illustration of the mass spectrometry for clusters isolated from electrolyte solutions. *E*: electric potential, *P*: pressure, Pt: platinum electrode, RP: rotary pump, TMP: turbo molecular pump.

clusters have been discussed on the basis of two proposed electrospray ionization models: the ion evaporation model (IEM)[29−31] and the charge residue model (CRM).[32] The correlation of the relative mass abundances with the solvation energy depending on ionic radius has been explained by IEM and the extended CRM.[26,27] Wang and Cole[26,27] reported that dependence of the relative abundances of the cluster ions on the solvation energy was absent in the case where two kinds of salt were mixed: the ions constituting the droplet charge excess were fixed and the counterions were varied, such as NaCl + NaI for the positive ion measurement and NaCl + KCl for the negative ion measurement. We think that this reported inconsistency with the solvation energy will be rationalized on the assumption that the ion−counterion interaction is competing with the ion−solvent interaction, as will be presented here. Since we do not have any direct experimental probes, we cannot discuss the electrospray ionization mechanism, such as IEM or CRM, in detail more than the previous reports. However, the complementary relation between the ion−counterion and the ion−solvent interactions, which is reported here, will provide insight into the electrospray ionization mechanism, too.

## Experimental Section

Mass spectrometric analyses of positively and negatively charged clusters generated from electrolyte solutions were carried out by means of a specially designed mass spectrometer. The experimental setup is shown schematically in Figure 1. The apparatus is composed of a homemade electrospray interface, a quadrupole mass filter (Extrel, C50), and a specially designed five-stage differentially pumped vacuum system. During the experiment, a methanolic solution of a lithium halide salt (LiCl, LiBr, or LiI) was injected into the high electric field between the nozzle and the first skimmer through a fused silica capillary tube (i.d. 0.1 mm) at a flow rate of 0.01 $cm^3$/min. Based on the electrospray principle, positively or negatively charged liquid droplets including excess cations or anions were generated, according to the polarity of the electric field. The resulting multi-charged liquid droplets entered into the second, third, and fourth chambers traveling under the influence of the potential and pressure gradients. The multi-charged liquid droplets were then fragmented into singly charged clusters via adiabatic expansion and electrostatic repulsion during their flight. The charged clusters, which reached the quadrupole mass filter, were mass-analyzed without further external ionization.

To minimize desolvation from solvated ion clusters, a pressure gradient from $P_1$ to $P_3$, shown in Figure 1, is held as small as possible to have moderate adiabatic expansion, and the electrospray nozzle is situated coaxial to the three skimmers to reduce collisional interactions. On the other hand, this specially designed nozzle-skimmer coaxial alignment makes the entering of nonionic (electrically neutral) species accompanied with ionic species increase, which causes the resolution of mass analyzer lower than the conventional apparatus, as a side effect. The resolution in the mass analysis was sacrificed to observe solvated species.

For obtaining the electrospray, electric voltage was supplied to the nozzle and three skimmers ($E_1-E_4$). It should be noted that the mass distribution is remarkably dependent on this electric voltage. March and co-workers[28] have already reported that the mass distribution of alkali metal chloride solutions are markedly influenced by the magnitude of "the cone voltage", which corresponds to the difference between $E_2$ and $E_3$ in our system. In their experiment, multi-charged clusters were observed at low cone voltage (around 10 V), which represents the initial distribution of ionic clusters without having energetic collisional interaction; whereas stable clusters such as magic-number species were observed at high cone voltages (around 70 V), which are formed through collisional dissociation. In our system, the resulting clusters were strongly dependent on the $E_2-E_3$ potential difference, as indicated by March et al., but its dependence was shown in a different way. At the small $E_2-E_3$ difference (around 10 V), singly charged solvated-ion clusters were observed; on the other hand, at the large $E_2-E_3$ difference (around 90 V), singly charged salt clusters without solvent molecules were observed. In comparing these results, we can say that the solvated-ion clusters are observed as the initial distribution of clusters without having collisional influence in our experiments at the small $E_2-E_3$ difference, and that the salt cluster formation is enhanced by the desolvation via collisional interaction at the large $E_2-E_3$ difference. Such a characteristic feature on our mass spectrometry is also due to the specially designed nozzle-skimmer alignment and the five-stage differentially pumped vacuum system. To have information on solvated ions, all the measurements were carried out in keeping with the $E_2-E_3$ difference $<10$ V, as listed in Table 1. The values of $E_1-E_4$ and $P_1-P_5$ are ones for a typical experiment, and all the measurements follow conditions similar to those shown in Table 1.

**TABLE 1: Values of Electric Voltages ($E_1$−$E_4$) and Pressures ($P_1$−$P_5$) for Positive and Negative Ion Measurements of 0.1 mol/dm$^3$ LiCl in Methanol**

| electric voltages (V) | positive ion | negative ion |
|---|---|---|
| $E_1$ | +3700 | −3800 |
| $E_2$ | +291 | −293 |
| $E_3$ | +293 | −295 |
| $E_4$ | +223 | −239 |
| **pressures (Torr)** | **positive ion** | **negative ion** |
| $P_1$ | 454.7 | 720 |
| $P_2$ | 9.53 | 14.6 |
| $P_3$ | $5 \times 10^{-3}$ | $8 \times 10^{-3}$ |
| $P_4$ | $1 \times 10^{-5}$ | $5 \times 10^{-5}$ |
| $P_5$ | $1 \times 10^{-6}$ | $3 \times 10^{-6}$ |

The nitrogen gas is necessary to maintain an appropriate pressure balance (from $P_1$ to $P_5$), and to prevent from discharging between the nozzle and the skimmers. To switch from positive-ion to negative-ion measurement, the polarity of the electric field was changed.

Chemicals of the highest purity were used without further purification: LiCl (anhydrous, special grade, Wako), LiBr (99+%, Aldrich), LiI (anhydrous, 99.999%, Aldrich), and $CH_3OH$ (special grade, Wako).

## Results and Discussion

**1. Positive Ion Clusters.** Figures 2, 3, and 4 show the mass spectra of positively charged clusters observed for the methanolic solutions including LiCl, LiBr, and LiI, respectively. The mass distribution of clusters is clearly dependent on the halide ion.

Figure 2, parts a and b, shows the mass spectra of clusters observed for the LiCl solutions at 0.001 and 0.1 mol/dm$^3$, respectively. At the lower concentration (0.001 mol/dm$^3$), two series of clusters are observed as a function of the number of methanol molecules. One series has a composition of $Li^+(CH_3OH)_n$, where $n = 1, 2, 3, \cdots$, which represents the solvated $Li^+$. The other series has a composition of $Li^+(Li^+Cl^-)(CH_3OH)_m$, where $m = 0, 1, 2, 3, \cdots$, which can be referred to as *solvated salt clusters* and contains solvated $Li^+$ ions interacting with an ion-pair unit, $Li^+Cl^-$ (*nonsolvated salt clusters* in the case of $m = 0$). At the higher concentration (0.1 mol/dm$^3$), as shown in Figure 2b, the intensities for the solvated salt clusters increase obviously, moreover, clusters including more than one unit of ion pairs, $Li^+(Li^+Cl^-)_s(CH_3OH)_m$, where $s = 1, 2, \cdots$, $m = 0, 1, 2, 3, \cdots$, become also observable clearly. This concentration dependence reasonably indicates that the probability of the ion-pair formation increases with an increase of the LiCl concentration.

The mass spectra of clusters observed for LiBr in methanol are shown in Figure 3. The solvated $Li^+$ clusters $Li^+(CH_3OH)_n$, and the solvated salt clusters $Li^+(Li^+Br^-)_s(CH_3OH)_m$, were detected, and the mass distributions were similar to those observed for LiCl as shown in Figure 2.

The clustering observed for LiI in methanol was clearly different from that for LiCl and LiBr. Figure 4 shows mass spectra of clusters observed for 0.001 and 0.1 mol/dm$^3$ LiI in methanol. The solvated $Li^+$ clusters, $Li^+(CH_3OH)_n$, and the solvated salt clusters, $Li^+(Li^+I^-)_s(CH_3OH)_m$, are observed, and the latter series of clusters becomes predominant at the higher concentration. This is the same concentration dependence as observed for LiCl and LiBr. However, the observed mass distribution, especially for the series of solvated salt clusters,

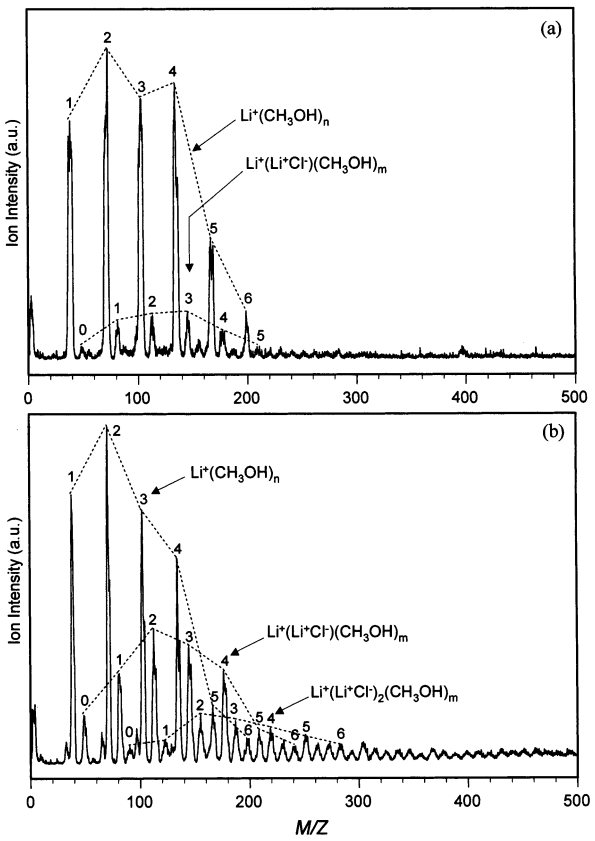


**Figure 2.** Mass spectra of positively charged clusters observed for LiCl in methanol at concentrations 0.001 mol/dm$^3$ (a) and 0.1 mol/dm$^3$ (b). The numbers above the peaks represent $n$ or $m$ for $Li^+(CH_3OH)_n$ or $Li^+(Li^+Cl^-)_s(CH_3OH)_m$, respectively. The assignment for $s \geq 3$ becomes difficult due to the overlapping closely with other peaks.

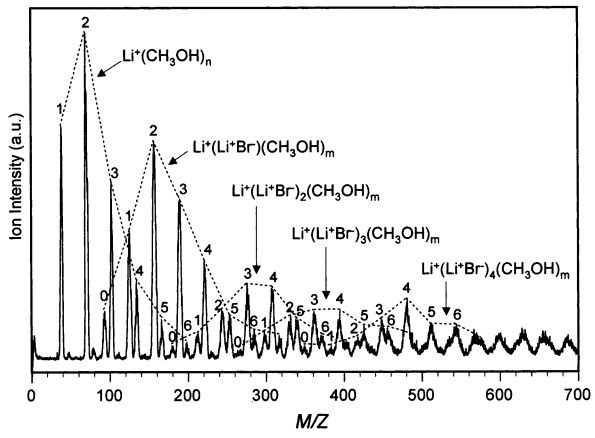


**Figure 3.** Mass spectra of positively charged clusters observed for LiBr (0.1 mol/dm$^3$) in methanol. The numbers above the peaks represent $n$ or $m$ for $Li^+(CH_3OH)_n$ or $Li^+(Li^+Br^-)_s(CH_3OH)_m$, respectively. The assignment for $s \geq 5$ becomes difficult due to high relative isotope abundance.

$Li^+(Li^+I^-)_s(CH_3OH)_m$, is quite different from that for $Li^+(Li^+Cl^-)_s(CH_3OH)_m$ and $Li^+(Li^+Br^-)_s(CH_3OH)_m$. For example, the numbers of methanol molecules $m$ forming stable structures of $Li^+(Li^+I^-)(CH_3OH)_m$ and $Li^+(Li^+I^-)_2(CH_3OH)_m$ are 6 and 7, respectively, as shown by the connected lines in Figure 4b. The $m$ value for the stable structure of $Li^+(Li^+I^-)_s(CH_3OH)_m$ increases with increase of the number of included ion pairs, $s$. $m$ increases from 5−6 to 7−8 when $s$ changes from 1 to 3. In contrast, the corresponding $m$ values for LiCl and LiBr solutions are much smaller. The mass distribution of $Li^+(Li^+I^-)_s(CH_3OH)_m$ clusters as a function of the number of

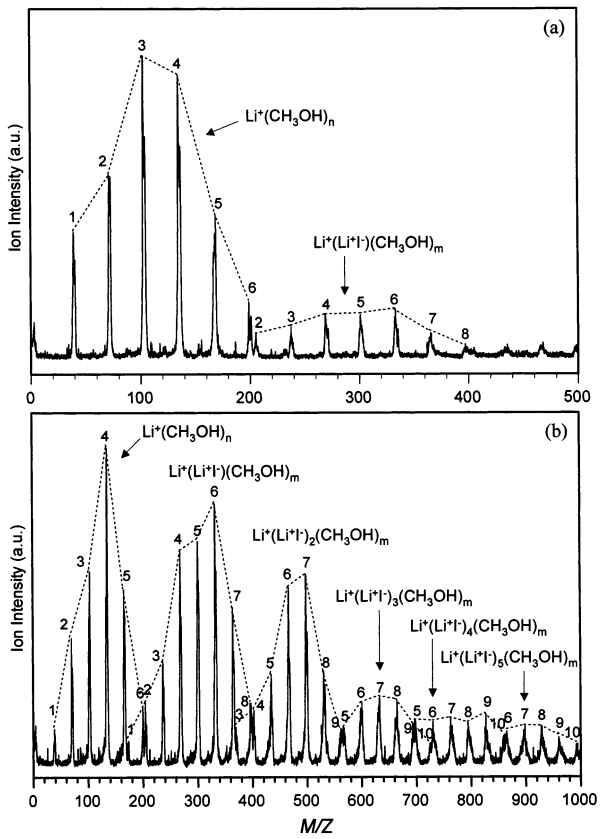


**Figure 4.** Mass spectra of positively charged clusters observed for LiI in methanol at concentrations 0.001 mol/dm$^3$ (a) and 0.1 mol/dm$^3$ (b). The numbers above the peaks represent $n$ or $m$ for $Li^+(CH_3OH)_n$ or $Li^+(Li^+I^-)_s(CH_3OH)_m$, respectively.

methanol molecules $m$ at a given $s$ is clearly different from that of $Li^+(CH_3OH)_n$ clusters as a function of $n$. On the other hand, for the LiCl− and LiBr−methanol solutions, the mass distributions of $Li^+(Li^+Cl^-)_s(CH_3OH)_m$ and $Li^+(Li^+Br^-)_s(CH_3OH)_m$ as a function of the number of methanol molecules $m$ at a given $s$ look similar to those of $Li^+(CH_3OH)_n$ as a function of $n$, which is witnessed by the connected lines in Figures 2 and 3.

As for the mass distribution of $Li^+(Li^+X^-)_s(CH_3OH)_m$, there is another important point concerning the formation of $Li^+(Li^+X^-)_s$ clusters without including any methanol molecules. The nonsolvated salt clusters: $Li^+(Li^+Cl^-)_s$ with $s = 1$ and 2 are clearly observed at the higher concentration (Figure 2b). It is difficult to identify the $Li^+(Li^+Cl^-)_s$ clusters with $s \geq 3$ because of overlap with other peaks. Similarly, $Li^+(Li^+Br^-)_s$ clusters are also observed for $s = 1$ and 2 clearly in Figure 3. On the other hand, nonsolvated $Li^+(Li^+I^-)_s$ clusters are hardly observed in Figure 4.

The mass spectrometric analyses for the positive ion clusters indicate that there is a complementary relation between a $Li^+-CH_3OH$ interaction and a $Li^+-X^-$ interaction. In the case of $X^- = Cl^-$ or $Br^-$, $Li^+-X^-$ interaction is relatively strong, which leads to the decrease of $Li^+-CH_3OH$ interaction. On the other hand, in the case of $X^- = I^-$, $Li^+-CH_3OH$ interaction is enhanced by the decrease of $Li^+-X^-$ interaction.

**2. Negative Ion Clusters.** The presented positively charged clusters were generated by the fragmentation of the positively charged liquid droplets, which extracted from electrolyte solutions by the electrospray method. Therefore, all clusters, observed in Figures 2, 3, and 4, include an excess number of $Li^+$ over the number of $X^-$. However, since positive and negative charges should be balanced precisely in solution just before the electrospray process is initiated, the analysis of negatively charged clusters is indispensable for having a real image of microscopic pictures about the clusters. Figures 5, 6, and 7 show the mass spectra of negatively charged clusters observed for methanol solutions including LiCl (0.001 mol/dm$^3$), LiBr (0.1 mol/dm$^3$), and LiI (0.1 mol/dm$^3$), respectively. Similarly to the positively charged clusters, the solvated $X^-$ clusters, $X^-(CH_3OH)_k$, and the negatively charged solvated salt clusters, $X^-(Li^+X^-)_p(CH_3OH)_r$, were observed in the mass spectra.

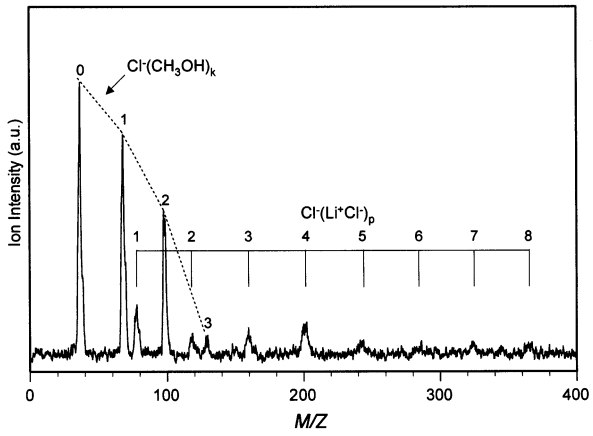


**Figure 5.** Mass spectra of negatively charged clusters observed for LiCl (0.001 mol/dm$^3$) in methanol. The numbers above the peaks represent $k$ or $p$ for $Cl^-(CH_3OH)_k$ or $Cl^-(Li^+Cl^-)_p$, respectively.

The number of solvating methanol $k$ of $X^-(CH_3OH)_k$ is 1, 2, or 3 for $X^- = Cl^-$ and $Br^-$, and 1 or 2 for $X^- = I^-$. The solvation for the relatively smaller anions, $Cl^-$ and $Br^-$, is stronger than that for the relatively larger anion, $I^-$. Furthermore, nonsolvated $Cl^-$, $Br^-$, and $I^-$ without including any solvent methanol molecules are observed as a prominent peak. An explanation for having such clusters might be a desolvation process, which will be accelerated in the case of weak solvation. If one compares the mass distributions for $X^-(CH_3OH)_k$ with those for $Li^+(CH_3OH)_n$ observed in Figures 2, 3, and 4, it is reasonable to conclude that the solvation for $Li^+$ by $CH_3OH$ is more favorable than for $X^-$ in these solutions. Bare $Li^+$ ion without solvating molecules was hardly observed, and the number of methanol molecules forming solvated $Li^+$, $n$ of $Li^+(CH_3OH)_n$, can be detected up to $n = 6$, as shown in Figures 2, 3, and 4.

As for the negatively charged salt clusters, $X^-(Li^+X^-)_p(CH_3OH)_r$, the mass distribution as a function of the number of methanol molecules, $r$, is also varying with the anions $X^-$. For LiCl solution (Figure 5), $Cl^-(Li^+Cl^-)_p(CH_3OH)_r$ clusters for $1 \leq p \leq 8$ were obviously formed without including any methanol molecules ($r = 0$). This is again a sign of a desolvation process due to weak solvation. On the other hand, for the LiI solution (Figure 7), $I^-(Li^+I^-)_p(CH_3OH)_r$ with $1 \leq p \leq 4$ were observed as accompanied by the solvating methanol molecules. Especially for $I^-(Li^+I^-)_p(CH_3OH)_r$ with $p \geq 3$, those with including methanol molecules become superior to the ones without methanol molecules ($r = 0$). The $CH_3OH$ molecules in $I^-(Li^+I^-)_p(CH_3OH)_r$ are thought to be localized around the $Li^+$, because the solvation for $I^-$ is so weak as described above. As for the solvated salt clusters with a negative charge, too, the complementary relation between a $Li^+-CH_3OH$ interaction and a $Li^+-X^-$ interaction is satisfied.

**3. A Simplified Model for Cluster Formation.** As observed herein the mass spectra, the solvated salt clusters were formed efficiently from the methanolic salt solution. This indicates that

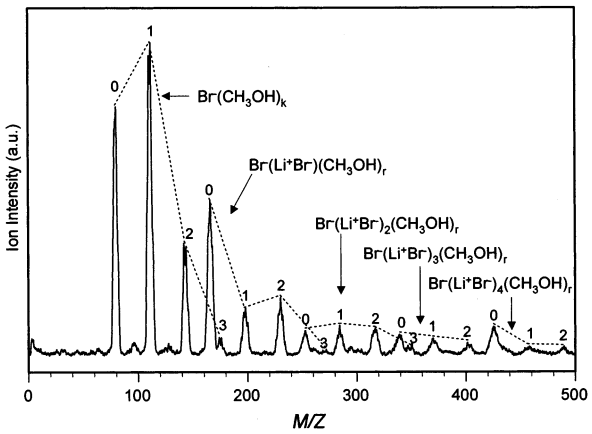


**Figure 6.** Mass spectra of negatively charged clusters observed for LiBr (0.1 mol/$dm^3$) in methanol. The numbers above the peaks represent $k$ or $r$ for $Br^-(CH_3OH)_k$ or $Br^-(Li^+Br^-)_p(CH_3OH)_r$, respectively.

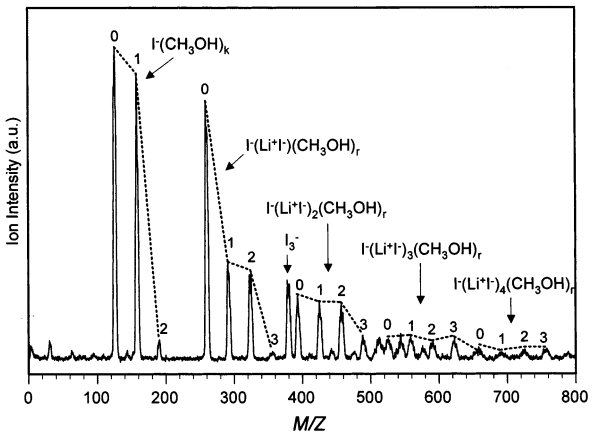


**Figure 7.** Mass spectra of negatively charged clusters observed for LiI (0.1 mol/$dm^3$) in methanol. The numbers above the peaks represent $k$ or $r$ for $I^-(CH_3OH)_k$ or $I^-(Li^+I^-)_p(CH_3OH)_r$, respectively. A part of $I^-$ was oxidized electrochemically to form $I_3^-$.

ion−counterion electrostatic interaction plays an important role in the cluster formation. To derive a simple cluster formation model, we assume that two types of interactions, an ion−solvent interaction and an ion−counterion interaction, will mainly contribute to the clustering.

The idea is that the solvated salt clusters are formed due to the balance between the $Li^+\cdots X^-$ electrostatic interaction and the ion−solvent interaction (solvation). In the case when the electrostatic interaction is superior to the solvation interaction, the contact ion pair will be stabilized. On the other hand, a solvent-separated ion pair will be formed favorably, when the $Li^+\cdots X^-$ electrostatic interaction is comparable with or inferior to the solvation interaction. On the basis of the present experimental results, we might say that LiCl and LiBr would have a tendency to form the (solvated) contact ion pairs, and that LiI would form the solvent-separated ion pairs, favorably. A sketch of the model is shown in Figure 8.

In case of the LiCl and LiBr, which include relatively small anions, the electrostatic interaction between $Li^+$ and $Cl^-$ or $Br^-$ is thought to be preferred to the $Li^+-CH_3OH$ (ion−solvent) interaction. When the $Li^+$ has an interaction with $Cl^-$ or $Br^-$, the solvation for $Li^+$ by methanol will be weakened, as shown in Figure 8a. In other words, the methanol molecules solvating $Li^+$ will be substituted by the $Cl^-$ and $Br^-$. Therefore, the $Li^+(Li^+Cl^-)(CH_3OH)_m$, for example, will have a composition in which the solvated $Li^+$ has interaction with the nonsolvated ion pair ($Li^+Cl^-$). On the other hand, the electrostatic force

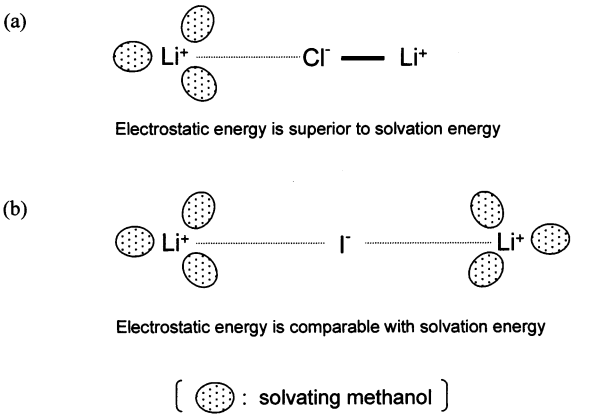


**Figure 8.** Schematic illustration for the possible ion-pair structure with positive charge. (a) A solvated $Li^+$ is interacting with a strong ion pair ($Li^+Cl^-$). (b) Solvated $Li^+$ ions are interacting with $I^-$.

**TABLE 2: Free Energies of Solvation of Ions by Methanol (1 atm gas → unit mole fraction solution): $\delta g_{sol}$ in kJ $mol^{-1}$ at 298 K[33]**

| cation | $\Delta G_{sol}$ | anion | $\Delta G_{sol}$ |
|---|---|---|---|
| $Na^+$ | −410.0 | $Cl^-$ | −270.7 |
| $K^+$ | −334.3 | $Br^-$ | −244.3 |
| $Rb^+$ | −313.0 | $I^-$ | −211.3 |
| $Cs^+$ | −281.6 | | |

between $Li^+$ and $I^-$ is weaker due to lower charge density of $I^-$ than $Cl^-$ and $Br^-$. The electrostatic energy of $Li^+\cdots I^-$ will become comparable with the solvation energy for $Li^+$, in fact, the solubility of LiI is high. The weaker electrostatic interaction between $Li^+$ and $I^-$ makes the influence on the solvation of $Li^+$ by $I^-$ smaller. For example, $Li^+(Li^+I^-)(CH_3OH)_6$, which is observed as a prominent peak in the series of $Li^+(Li^+I^-)(CH_3OH)_m$ clusters in Figure 4b, will have the composition that two solvated $Li^+$ ions interact with $I^-$, as shown in Figure 8b. The structure of linear $Li^+\cdots I^-\cdots Li^+$ with which methanol interacts at $Li^+$ sides only is in good agreement with the geometrical forms which have already been calculated for $(Li_2I)^+(CH_3OH)_m$ with $m = 3$ and 4.[4]

**4. Comparing with Solvation Energy, Molar Conductivity, and Solvation Numbers.** To see a correlation between the observed cluster structures and the solution properties, here we would like to compare our results with solvation energy, molar conductivity, and solvation number data.

*i. Solvation Energy*. Free energy change for solvation of ions by methanol, $\Delta G_{sol}$, are listed in Table 2.[33] For both positive and negative ions, the stabilization by solvation ($|\Delta G_{sol}|$) increases with decrease of the ionic radius, that is, with increase of the charge density of ion. It is reasonably accepted that the $|\Delta G_{sol}|$ for $Li^+$ should be larger than that for $Na^+$. Accordingly, the $|\Delta G_{sol}|$ for $Li^+$ is much larger than that for the counteranions. These solvation energies are well reflected in the observed mass distributions. The solvated $Li^+$, $Li^+(CH_3OH)_n$: $1 \le n \le 6$, is observed as prominent species for LiCl, LiBr, and LiI solutions, but nonsolvated $Li^+$ is hardly observed for any solutions, as shown in Figures 2−4. On the other hand, nonsolvated $Cl^-$, $Br^-$, and $I^-$ are observed as prominent peaks for each negative ion mass spectrum (Figures 5−7). The solvent methanol is vaporized from the solvated anions more easily than from the solvated $Li^+$, which is in correlation with the $|\Delta G_{sol}|$. The mass distribution of the solvated $Cl^-$, $Br^-$, and $I^-$ shown in Figures 5−7 also have a correlation with the $|\Delta G_{sol}|$.

*ii. Molar Conductivity*. Salt clusters and their solvated ones are observed in each mass spectrum. This indicates that the ion−

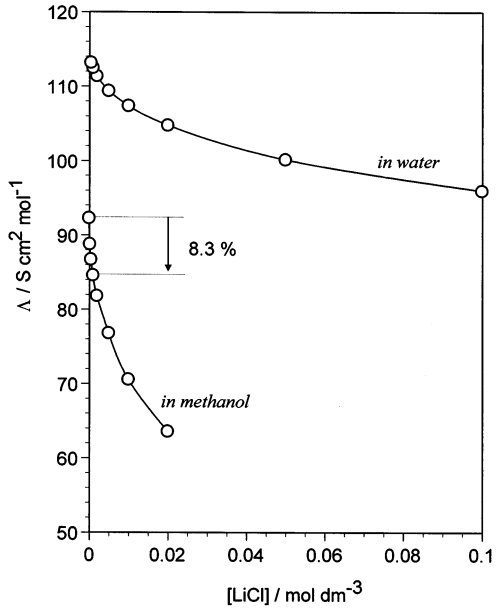


**Figure 9.** Plots of molar conductivities (Λ) of LiCl in water and in methanol as functions of LiCl concentration.[34]

counterion interaction is not negligible even at a lower concentration studied here. Such an ion−counterion interaction should be reflected in molar conductivities (Λ), which have already been demonstrated in our previous reports.[24,25] Figure 9 shows molar conductivities of LiCl in water and methanol as functions of LiCl concentrations.[34] The molar conductivies in water are nearly constant, whereas those in methanol decrease markedly with increase of the concentration, especially at lower concentrations. The ratio of a molar conductivity at 0.001 mol/dm$^3$ ($\Lambda_{0.001}$) to that at infinite dilution ($\Lambda_0$), $\Lambda_{0.001}/\Lambda_0$, in water is 0.977; while $\Lambda_{0.001}/\Lambda_0$ in methanol is 0.917. This indicates that the degree of ionization in methanol is obviously lower than that in water at this concentration.

The value of $\Lambda_{0.001}/\Lambda_0$ in methanol, 0.917, was found to be in correlation with the cluster structures observed for 0.001 mol dm$^{-3}$−LiCl in methanol (Figure 2a). In Figure 2a, $Li^+(CH_3OH)_n$ and $Li^+(Li^+Cl^-)(CH_3OH)_m$ are mainly observed. Each $Li^+(CH_3OH)_n$ includes one free $Li^+$, and each $Li^+(Li^+Cl^-)(CH_3OH)_m$ includes one $Li^+$ free from $Cl^-$ and one $Li^+$ bound to $Cl^-$. If these observed clusters are generated from the solvated ions and the ion pairs in the solution, the ratio presented by eq 1 should be related to the molar conductivities.

$$R_{\text{free}} = \frac{\sum \text{Li}_{\text{free}}}{\sum \text{Li}_{\text{free}} + \sum \text{Li}_{\text{bound}}} \quad (1)$$

$$\sum \text{Li}_{\text{free}} = \sum_n I\text{Li}^+(\text{CH}_3\text{OH})_n + \sum_m I\text{Li}^+(\text{Li}^+\text{Cl}^-)(\text{CH}_3\text{OH})_m \quad (2)$$

$$\sum \text{Li}_{\text{bound}} = \sum_m I\text{Li}^+(\text{Li}^+\text{Cl}^-)(\text{CH}_3\text{OH})_m \quad (3)$$

where $\sum \text{Li}_{\text{free}}$ and $\sum \text{Li}_{\text{bound}}$ represent the number of $Li^+$ free from $Cl^-$ and the number of $Li^+$ bound to $Cl^-$, respectively, and where $\sum_n I\text{Li}^+(\text{CH}_3\text{OH})_n$ and $\sum_m I\text{Li}^+(\text{Li}^+\text{Cl}^-)(\text{CH}_3\text{OH})_m$ represent the sum of the peak intensities of $Li^+(CH_3OH)_n$ and $Li^+(Li^+Cl^-)(CH_3OH)_m$ observed in Figure 2a, respectively. The $R_{\text{free}}$ value calculated through eqs 1−3 for Figure 2a was 0.89, what is close to the $\Lambda_{0.001}/\Lambda_0$ value, 0.917. This correlation indicates that the formation of the solvated ions and the salt clusters is related with the ion−solvent and the ion−counterion interactions in a solution.

*iii. Solvation Numbers.* Neutron diffraction studies of LiCl and LiBr in water and methanol have been extensively carried out, and both the solvent and the concentration effects on the solvation (or coordination) numbers for ions have been reported.[35−37] As for the solvent effect,[35] the solvation (coordination) number of $Cl^-$, 5.8 in $D_2O$ was decreased to 3.6 in methanol, which suggests that ion association is promoted in the concentrated methanol solution. On the other hand, looking at the concentration effect,[36,37] the hydration numbers of $Li^+$ in aqueous LiCl and LiBr solutions were changed from about 6 to about 3, as their concentrations changed from 2.0 to 25 mol %. This concentration effect also suggests that ion-pair formation occurs at higher concentrations. The effects of solvent and concentration on ion-pair formation are also confirmed in our mass specrometry. Furthermore, it should be noted that these solvation numbers in methanol estimated from the neutron diffraction experiments (6 for $Li^+$ and 3.6 for $Cl^-$) are in good correlation with the maximum solvation numbers estimated from the sequences of $Li^+(CH_3OH)_n$ and $Cl^-(CH_3OH)_k$ in Figures 2b and 5, respectively ($n = 6$ and $k = 3$).

The correlations of the results of mass spectrometric analyses of clusters with above-mentioned physicochemical properties of solutions indicate that the discussion of the observed clusters is significant; however, we must consider that the relatively weakly interacting molecules are vaporized during the fragmentation of liquid droplets into clusters. Moreover, the complementary relation between an ion−counterion interaction and an ion−solvent interaction has been recognized as an intrinsic property of solution. Here we reported that this complementary relation worked as a key factor to determine the structures of solvated ions and ion pairs in methanol solutions containing lithium halides.

**Acknowledgment.** The authors thank Prof. Gábor Pálinkás and Prof. Yasuo Kameda for helpful discussion. T.R. and T.M. are grateful for the invitation by National Institute of Advanced Industrial Science and Technology (AIST) as guest researchers. A.W. thanks Ms. Tsutae Yao for making arrangements of this international cooperation.

## References and Notes

(1) Ohtaki, H.; Radnai, T. *Chem. Rev.* **1993**, *93*, 1157−1204.
(2) Johansson, G. *Acta Chem. Scand.* **1989**, *43*, 307−321.
(3) Kunz, W.; Turq, P.; Barthel, J. *Ann. Phys. Fr.* **1990**, *15*, 447−491.
(4) Martin, T. P.; Bergmann, T. *J. Phys. Chem.* **1987**, *91*, 2530−2533.
(5) Hiraoka, K.; Misuse, S. *Chem. Phys.* **1987**, *118*, 457−466.
(6) Yamdagni, R.; Payzant, J. D.; Kebarle, P. *Can. J. Chem.* **1973**, *51*, 2507−2511.
(7) Hiraoka, K.; Mizuse, S.; Yamabe, S. *J. Phys. Chem.* **1988**, *92*, 3943−3952.
(8) Nielsen, S. B.; Masella, M.; Kebaric, P. *J. Phys. Chem. A* **1999**, *103*, 9891−9899.
(9) Radnai, T.; Kálmán, E.; Pollmer, K. *Z. Naturforsch* **1984**, *39a*, 464−470.
(10) Ohtaki, H. *Pure Appl. Chem.* **1987**, *59*, 1143−1150.
(11) Cartailler, T.; Kunz, W.; Turq, P.; Bellisent-Funel, M.-C. *J. Phys.: Condens. Matter* **1991**, *3*, 9511−9520.
(12) Johansson, G. *Adv. Inorg. Chem.* **1992**, *39*, 159−223.
(13) Nishi, N.; Yamamoto, K. *J. Am. Chem. Soc.* **1987**, *109*, 7353−7361.
(14) Yamamoto, K.; Nishi, N. *J. Am. Chem. Soc.* **1990**, *112*, 549−558.
(15) Wakisaka, A.; Carime, H. A.; Yamamoto, Y.; Kiyozumi, Y. *J. Chem. Soc., Faraday Trans.* **1998**, *94*, 369−374.
(16) Wakisaka, A.; Takahashi, S.; Nishi, N. *J. Chem. Soc., Faraday Trans.* **1995**, *91*, 4063−4069.
(17) Wakisaka, A.; Komatsu, S.; Usui, Y. *J. Mol. Liq.* **2001**, *90*, 175−184.

(18) Shin, D.; Wijnen, J. W.; Engberts, J. B. F. N.; Wakisaka, A. *J. Phys. Chem. B* **2001**, *105*, 6759−6762.
(19) Oguchi, T.; Wakisaka, A.; Tawaki, S.; Tonami, H.; Uyama, H.; Kobayashi, S. *J. Phys. Chem. B* **2002**, *106*, 1421−1429.
(20) Wakisaka, A.; Yamamoto, Y.; Akiyama, Y.; Takeo, H.; Mizukami, F.; Sakaguchi, K. *J. Chem. Soc., Faraday Trans.* **1996**, *92*, 3339−3346.
(21) Wakisaka, A.; Akiyama, Y.; Yamamoto, Y.; Engst, T.; Takeo, H.; Mizukami, F.; Sakaguchi, K.; Jones, H. *J. Chem. Soc., Faraday Trans.* **1996**, *92*, 3539−3544.
(22) Mochizuki, S.; Usui, Y.; Wakisaka, A. *J. Chem. Soc., Faraday Trans*. **1998**, *94*, 547−552.
(23) Wakisaka, A.; Watanabe, Y. *J. Phys. Chem. B* **2002**, *106*, 899−901.
(24) Kobara, H.; Wakisaka, A.; Takeuchi, K.; Ibusuki, T. *J. Phys. Chem. A* **2002**, *106*, 4779−4783.
(25) Mochizuki, S.; Wakisaka, A. *J. Phys. Chem. A* **2002**, *106*, 5095−5100.
(26) Wang, G.; Cole, R. B. *Anal. Chem*. **1998**, *70*, 873−881.
(27) Wang, G.; Cole, R. B. *Anal. Chim. Acta* **2000**, *406*, 53−65.
(28) Hao, C.; March, R. E.; Croley, T. R.; Smith, J. C.; Rafferty, S. P. *J. Mass Spectrom*. **2001**, *36*, 79−96.
(29) Iribarne, J. V.; Thomson, B. A. *J. Chem. Phys*. **1976**, *64*, 2287−2294.
(30) Thomson, B. A.; Iribarne, J. V. *J. Chem. Phys*. **1979**, *71*, 4451−4463.
(31) Fenn, J. B. *J. Am. Soc. Mass Spectrom*. **1993**, *4*, 524−535.
(32) Dole, M.; Mack, L. L.; Hines, R. L.; Mobley, R. C.; Ferguson, L. D.; Alice, M. B. *J. Chem. Phys*. **1968**, *49*, 2240−2249.
(33) Abraham, M. H.; Liszi, J. *J. Chem. Soc., Faraday Trans. 1* **1978**, *74*, 1604−1614.
(34) *Handbook of Chemistry (Kagaku-binran Kisohen 4th ed.)*; Japanese Chemical Society, Ed.; Maruzen: Tokyo, 1993; pp II-445−II-454.
(35) Yamagami, M.; Wakita, H.; Yamaguchi, T. *J. Chem. Phys*. **1995**, *103*, 8174−8178.
(36) Kameda, Y.; Usuki, T.; Uemura, O. In *High-Temperature Materials and Processes*; Rosen, A., Waseda, Y., Eds.; **1999**, *18*, 27−40.
(37) Kameda, Y.; Ebata, H.; Usuki, T.; Uemura, O. *Physica B* **1995**, *213 & 214*, 477−479.